Orthopaedics & Traumatology: Surgery & Research 105 (2019) 361–367

Contents lists available at ScienceDirect

Orthopaedics & Traumatology: Surgery & Research

journal homepage: www.elsevier.com

Original article

Computed tomography method for characterising the zebrafish spine

Laura Marie-Hardy[a,*], Marc Khalifé[a], Lofti Slimani[b], Hugues Pascal-Moussellard[a]

[a] Service d'orthopédie et de traumatologie, hôpital de la Pitié-Salpêtrière, 47, boulevard de l'hôpital, 75013 Paris, France
[b] EA2496, pathologie, imagerie & biothérapies orofaciales, faculté de chirurgie dentaire, université Paris Descartes, 1, rue Maurice-Arnoux, 92120 Montrouge, France

ARTICLE INFO

Article history:
Received 6 October 2018
Accepted 6 December 2018

Keywords:
Zebrafish
Computed tomography
Spine
Scoliosis
Live imaging

ABSTRACT

Background: The zebrafish is widely used in research due in part to its readily manipulable genome. Zebrafish models of spinal deformities including scoliosis were developed recently. However, the methods used to assess the spine in these models vary across studies. The primary objective of this study was to investigate the feasibility and modalities of local and regional spine structure evaluation by micro-CT in the normal zebrafish. The secondary objectives were to assess the feasibility of spinal angle measurements in normal zebrafish subjected to external stresses designed to mimic spinal deformities, to determine normal angle values in the coronal and sagittal planes, and to detail the micro-CT features of the zebrafish spine.
Hypothesis: Micro-CT is an effective and reproducible tool for determining orthopaedic parameters to characterise the zebrafish spine.
Material and Methods: Two observers conducted preliminary analyses on 15 zebrafish including 12 adults (aged 18 months) and 3 juveniles (aged 12 weeks). For the analyses, 6 of the animals were placed in an artificial position to mimic a scoliosis spinal deformity. Micro-CT (Quantum FX Caliper™) was used with 59 μm resolution and a 30-mm field of view. Image processing was with RadiAnt DICOM Viewer™ software.
Results: We defined several assessment planes on the 3D micro-CT reconstructions to measure orthopaedic parameters in the sagittal plane (thoracic and maximal kyphotic curves with their apices, length of the various spinal segments, and sagittal index) and coronal plane (Cobb angles, apices, end-vertebrae, coronal alignment, and side of the convexity). Mean thoracic kyphosis was 20.5°±5.0° in the adults and 8.7° in the juveniles. No curvature was apparent in the coronal plane in the zebrafish left in the neutral position. In the zebrafish with artificially induced curves, micro-CT was effective in determining the Cobb angles and apical vertebrae.
Discussion: This work defines a standardised micro-CT method for assessing the zebrafish spine. In addition, spinal parameter values that can be considered normal were determined, namely, less than 30° of thoracic kyphosis in the sagittal plane and less than 10° in the coronal plane. Our method was effective in assessing induced spinal deformities on micro-CT reconstructions. We hope it will prove of value in future studies of the zebrafish model.
Level of evidence: IV.

1. Introduction

The zebrafish is among the animal models most widely used in scientific research, due to its easily manipulable genome that shares 70% of genes with humans [1,2]. The first zebrafish studies done in the 1960s focussed on pharmacological and toxicological issues. Since then, the zebrafish model has found uses in all the fields of biomedical research, notably development and genetics [3,4].

Compared to other vertebrates, the absence of limbs in fish is an advantage when seeking to study the normal or abnormal spine. Animal models used to investigate scoliosis, for instance, often involve surgical procedures such as spinal elongation in pigs [5] or limb amputation in mice [6]. Such models may therefore have limited relevance to human pathophysiology, as pointed out by Ouellet and Odent [7]. Several zebrafish models of spinal deformity were reported recently, including the *cfap298* or kurly mutant and the *pkd2l1* mutant, both characterized by a scoliosis-like deformity

* Corresponding author.
E-mail address: l.mariehardy@gmail.com (L. Marie-Hardy).

https://doi.org/10.1016/j.otsr.2018.12.008
1877-0568/

[8,9]. The scoliosis-like 3D spinal deformity described in *pkd2l1* mutants by Boswell and Ciruna suggests a role as a model of idiopathic scoliosis [10,11].

Characterising spinal deformities in fish can be challenging, however, for reasons including the small size of the animal, differences in spinal morphology, and the use of inappropriate assessment techniques such as photographs and immunohistochemistry. Micro-computed tomography (μCT) is increasingly used to detect vertebral deformities. In contrast, μCT has only rarely been used to characterise spinal curves by measuring angles, assessing sagittal and coronal alignment, and identifying apical vertebrae [12,13].

The primary objective of this study was to investigate the feasibility and modalities of local and regional spine structure evaluation by μCT in the normal zebrafish. The secondary objectives were to assess the feasibility of spinal angle measurements in normal zebrafish subjected to external stresses designed to mimic spinal deformities, to determine normal angle values in the coronal and sagittal planes, and to detail the μCT features of the zebrafish spine. The working hypothesis was that μCT was an effective and reproducible tool for determining orthopaedic parameters to characterise the zebrafish spine.

2. Material and Methods

A cohort study was performed in zebrafish (*Danio rerio*) raised in the PHENO-ZFish department of the brain and spinal cord institute (ICM) in Paris, France. Housing conditions complied with current European regulations. The animals were raised in 20-L aquariums filled with water at 25 °C, with no more than 20 animals in each aquarium. Veterinarians monitored the fish once a week. The study protocol was approved by the appropriate ethics committee (APAFiS procedure, #2018071217081175). The study population comprised 15 wild-type zebrafish including 12 adults (aged 18 months) and 3 juveniles (aged 12 weeks). The animals were free of gene mutations.

In preliminary studies, standard radiography, mammography machine imaging, and dental radiographs failed to provide assessable images. We therefore turned to μCT to image the spines of the animals. CT machines used in humans are not suitable for imaging animals as small as zebrafish. For this reason, and to avoid hygiene issues, we used a small-animal imaging platform. The μCT machine was a Quantum FX Caliper™ (PerkinElmer, Caliper Life Sciences, Hopkinton, MA, USA). Acquisition was with 59 μm resolution and a 30-mm field of view. Acquisition required 3 minutes in the adults and 2 minutes in the smaller juveniles. Each animal was anesthetised and placed in an appropriately sized Petri dish containing water to ensure survival and to avoid potential positioning artefacts due to contact with a hard surface or to positioning within a gel. Rigaku™ software (Rigaku, Tokyo, Japan) was used for real-time 3D reconstruction and RadiAnt DICOM Viewer™ (Medixant, Poznán, Poland) for image processing.

The first 6 adult zebrafish were imaged after euthanasia with tricaine mesylate MS-222 0.2% for 10 minutes. The other 6 adults and the 3 juveniles underwent μCT after general anaesthesia with tricaine mesylate MS-222 0.02% diluted in the water filling the Petri dish. The duration of the anaesthesia was 15 minutes, e.g., the sum of the transfer time and of the imaging time. The water was then changed and the animals monitored until fully awake. In the 6 euthanised adults, polystyrene cylinders were positioned in contact with the body to create artificial spinal curves.

To assess measurement reproducibility, two independent observers used our study method to measure thoracic kyphosis in 10 animals. Pearson's correlation coefficient between the two measured values was computed using XLSTAT™ (Microsoft, Redmond, WA, USA). For the assessment, the spine was divided into three segments: the thoracic segment composed of the rib-bearing vertebrae, the lumbar segment extending from the thoracic segment down to the caudal fin, and the cervical segment extending from the cranio-cervical junction to the first thoracic vertebra.

3. Results

No technical difficulties arose while acquiring the μCT scans. Of the 9 anaesthetised animals, none experienced side effects due to the anaesthetic. Several phases were defined for the analysis of the 3D reconstructions.

4. The μCT method

4.1. Phase 1: image processing

A bony window was used for μCT acquisition to visualise only the skeleton. The next step was 3D reconstruction. Finally, the fins were subtracted to avoid their interfering with the evaluation (Fig. 1).

4.2. Phase 2: evaluation in the sagittal plane

First, the 3D reconstruction was oriented based chiefly on superimposition of the two ocular globes and of the ribs in each pair (Figure 1). Once proper sagittal orientation was thus achieved, the total length of the zebrafish was measured. To eliminate effects of soft tissue (dorsal fin) variability, the sagittal axis of the zebrafish was defined as the line drawn from the tip of the jaw to the centre of the most caudad vertebra (Fig. 2A). The following sagittal parameters were then determined.

Cobb's technique was used to measure the angles of each of the following kyphotic curves (Fig. 2):

- thoracic kyphotic curve, between the proximal and distal ends of the spine segment bearing the ribs;
- maximal kyphotic curve, between the proximal and distal ends of the longest kyphotic curve.

The vertebra at the apex of each curve was identified.

The sagittal index of the maximal kyphotic curve was then computed as the length of the line segment starting at the centre of the apical vertebra and dropped down perpendicularly to the sagittal axis over the length of the line from the tip of the jaw to the last vertebra, normalised for the length of the zebrafish (Fig. 2B); if the animal had several sagittal curves, the sagittal index was computed also for the other kyphotic or lordotic curves.

The length of each segment was measured (mm), with the thoracic segment defined as the rib-bearing vertebrae; the lumbar segment as the vertebrae distal to the thoracic segment; and the cervical segment as the vertebrae between the cranio-cervical junction and the proximal facet joint of the first thoracic vertebra, which was easier to visualise and therefore to measure on the coronal reconstructions (Fig. 3).

4.3. Phase 3: evaluation in the coronal plane

Alignment was assessed based on three criteria: symmetry of the arch-shaped jaw, symmetry of the nasal sinuses, and parallel orientation of the ribs in either side of the spine (Fig. 3, top). The coronal axis was defined as the line drawn from the middle of the tip of the jaw to the centre of the first thoracic vertebra (Fig. 3, middle). As an additional means of ensuring proper orientation of the animal, we checked that the total lengths in the coronal and

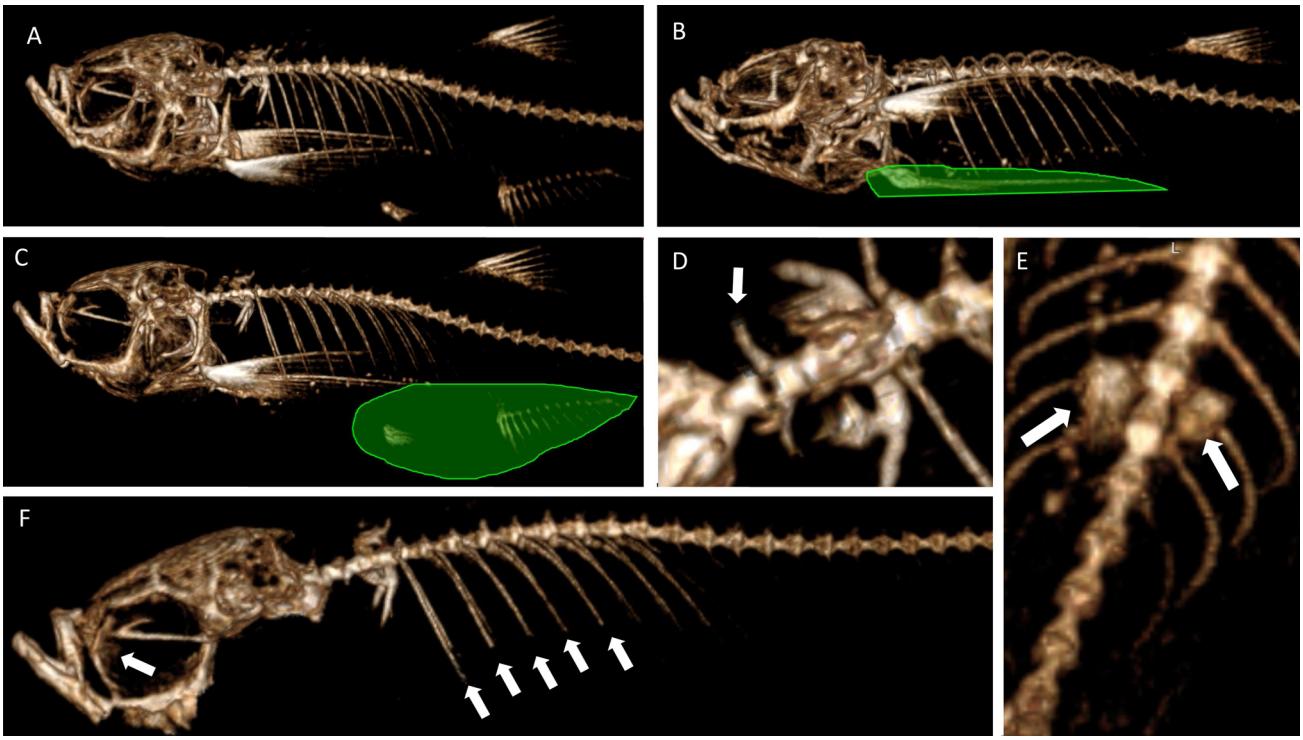

Fig. 1. First step of μCT imaging. A. Bony windowing is essential to optimise visualisation of the skeleton. B and C. The cartilaginous structures such as fins were subtracted to avoid their interfering with the visualisation of the spine. D. The cervical spine was emphasised to ensure good visibility of the transverse processes (white arrow). E. Example of poor bony windowing: the vertebrae are blurry and the organs are still visible (arrows). F. Image ready for evaluation in the sagittal plane: the ocular globes are aligned (arrows), the rib in each pair are superimposed (arrows), and the cervical spine is clearly visible.

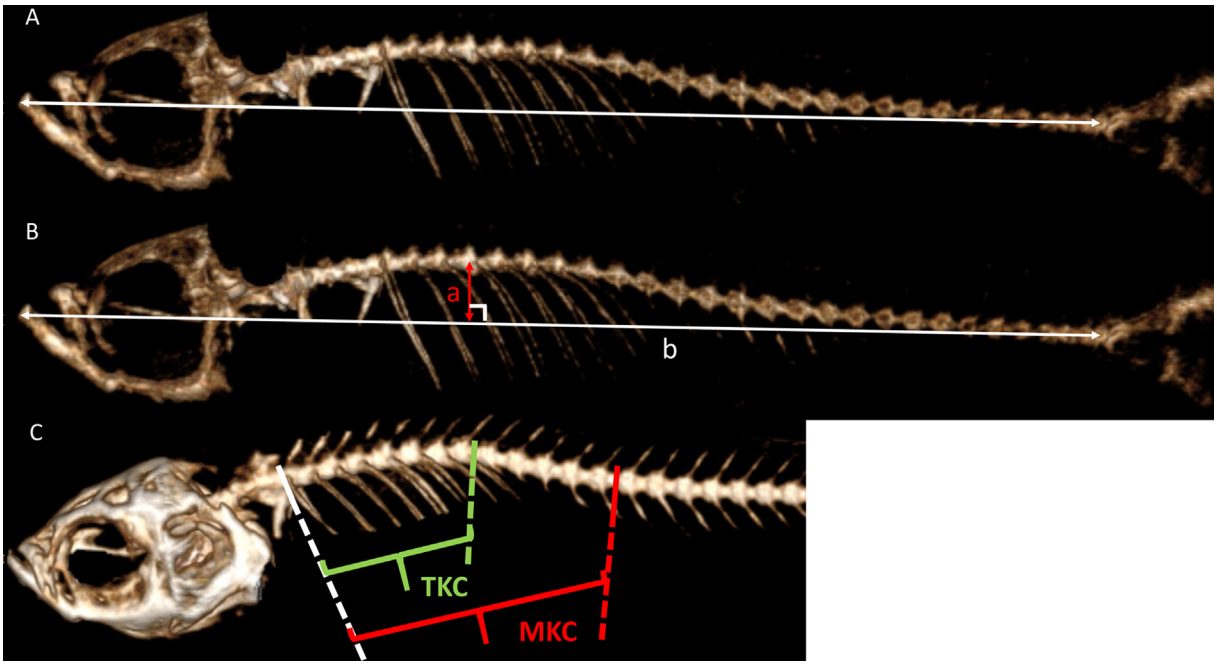

Fig. 2. Evaluation in the sagittal plane. A. Sagittal axis: line connecting the tip of the jaw to the centre of the last vertebra. B. Sagittal thoracic kyphosis index: a/b ratio. C. Angle measurements of the thoracic kyphotic curve (TKC, green) and maximal kyphotic curve (MKC, red).

sagittal planes were consistent. If the difference was greater than 3%, the orientation manoeuvres were repeated.

The following were identified on the coronal reconstructions:

- presence, number, and location (thoracic and/or lumbar) of spinal curves;
- side of the convexity of the major curve (right or left);
- Cobb angle values of each curve in the coronal plane;
- coronal malalignment (mm), defined as the length of the line segment starting at the centre of the most distal vertebra and dropped perpendicularly to the coronal axis; normalising this value for the length of the animal produced a parameter that

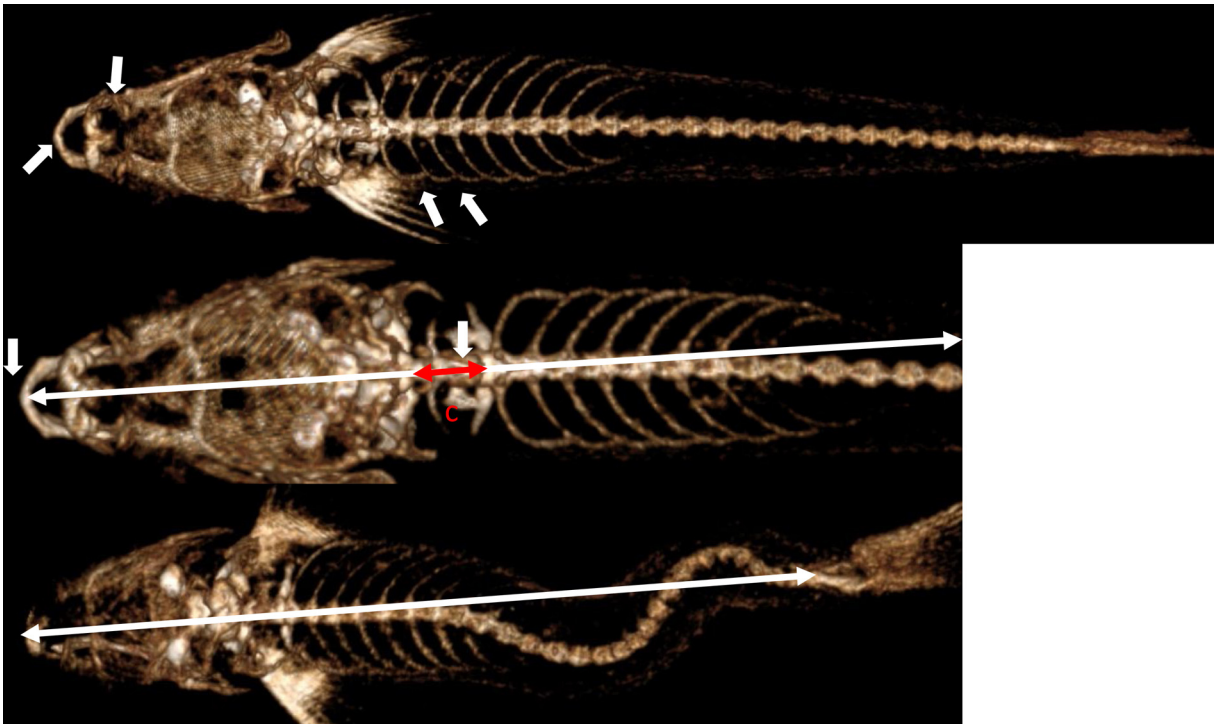

Fig. 3. Evaluation in the coronal plane. Top: the jaw (white arrow on the left) and nasal sinuses (next white arrow) are symmetrical and the ribs on each side of the spine are parallel to one another (parallel white arrows). Middle: coronal axis (white) from the tip of the jaw (white arrow on the left) to the centre of the first thoracic vertebra (white arrow in the middle); measurement of the length of the cervical segment from the cranio-cervical junction to the first thoracic vertebra (red arrow). Bottom: despite the curves induced in this animal, overall coronal alignment is preserved (coronal malalignment is 0 mm).

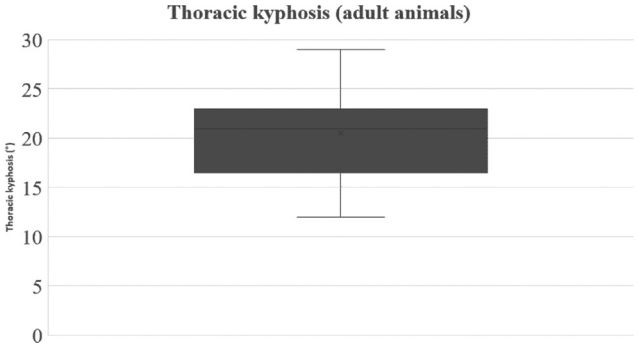

Fig. 4. Box plot of values (minimum and maximum, first and third quartiles, median, and mean [X], in degrees) of the thoracic kyphotic curve angles in the adult zebrafish.

was independent from animal size, thereby allowing comparisons across cohorts (Fig. 3).

5. Measurement results

Measurements were performed in 12 adult zebrafish (aged 18 months), 8 females and 4 males, and in 3 juvenile zebrafish (aged 12 weeks), 2 males and 1 female. Mean total length was 31.5 ± 1.88 mm (range, 29.0–35.6 mm) in the adults and 19.7 (range, 19.2-20.1 mm) in the juveniles. Mean thoracic kyphosis was 20.5°±5.0° (range, 12°–29°) in the adults and 8.7° (range, 5°–12°) in the juveniles (Fig. 4). In the coronal plane, in the adults, the mean curve was 2.4°±3.2°, none of the curves exceeded 10°, and the most marked curve was 8°. Of the 4 adults with coronal curves greater than 5°, two had the apex at T9, 1 at T8, and 1 at L2. None of the other animals in the cohort exhibited coronal malalignment. Mean length of the cervical segment in the adults was 1.81 ± 0.56 mm (range, 1.35–2.02 mm).

Two observers independently measured the kyphotic curves in a subgroup of 10 zebrafish including adults and juveniles (Fig. 5). Pearson's interobserver correlation coefficient was 0.98.

5.1. Measurement results in the animals with induced spinal curves

One or two polystyrene cylinders were used to induce spinal curves in 6 adults (Fig. 6). The mean Cobb angle of the major curve in these animals was 62.2°±7.1 (range, 52°–71°). Pearson's interobserver correlation coefficient was 0.97.

5.2. Spinal morphology

Neural and hemal arches were visible on either side of the vertebral bodies (Fig. 7). No vertebral deformities were detected in any of the animals. The inter-vertebral discs were not seen with sufficient clarity to allow characterisation.

Each of the 12 adults had 2 cervical vertebrae. Mean number of thoracic and lumbar vertebrae in the 12 adults was 8.5 and 16, respectively (Table 1).

Table 1
Number of vertebrae and lengths of the cervical, thoracic, and lumbar spinal segments.

	Cervical	Thoracic	Lumbar
Number of vertebrae, mean ± SD (range)	2 ± 0 (2–2)	8.5 ± 0.8 (7–10)	17.1 ± 1.2 (15–19)
Length, mm, mean ± SD (range)		0.79 ± 0.1 (0.65–0.97)	0.71 ± 0.1 (0.47–0.96)

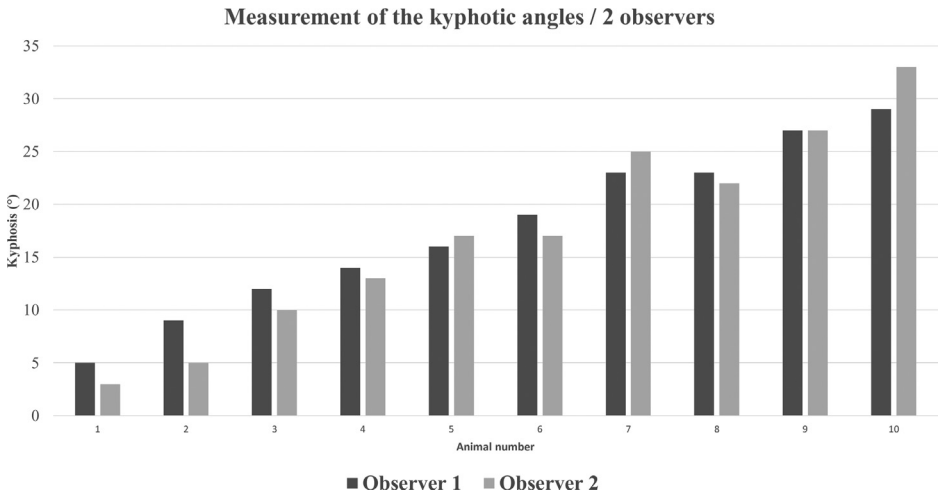

Fig. 5. Histogram of Cobb angle values of the thoracic kyphotic curves (TKC) measured on 3D reconstructions by two independent observers.

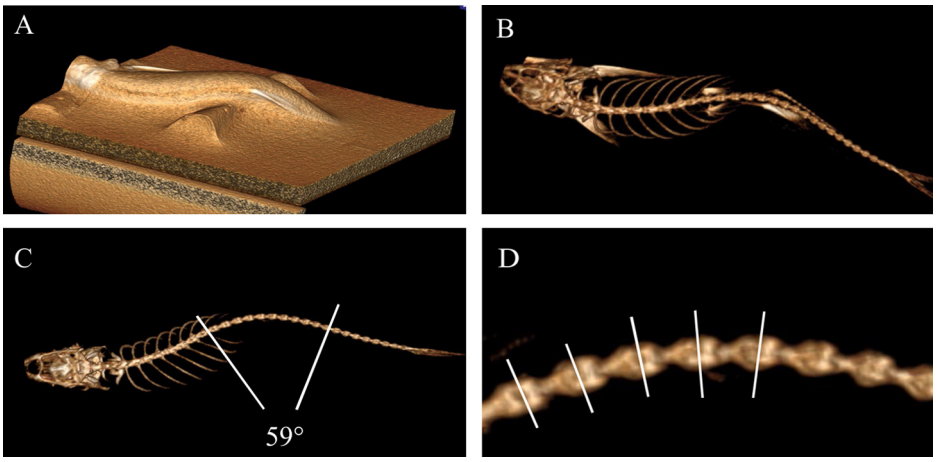

Fig. 6. Evaluation of artificially induced curves. A. Installation of the animal on a polystyrene cylinder. B. Bony windowing in the same plane as for image A. C. The Cobb angle of the major curve is 59°. D. Detail of reconstruction with each of the inter-articular lines.

6. Discussion

In a cohort of zebrafish, our μCT method provided good-quality segmental and global assessments of the spine, thereby allowing us to obtain reproducible measurements (with inter-observer correlation coefficients above 0.95). These results confirm our working hypothesis. The 3D reconstruction of μCT images provides a circumferential assessment of the vertebras. In addition, our method allows live imaging and may therefore hold promise for monitoring zebrafish throughout growth, thereby providing additional information compared to other methods such as studies of fixed tissues stained using alizarin red to assess skeletal development [14]. CT is the reference standard for imaging bone tissue. Thus, our μCT spinal assessment method provides better resolution compared to the optical methods that were used to establish zebrafish anatomy atlases [15,16]. In addition, our spinal morphology findings are consistent with previously published data [17,18].

Values that can be considered normal in zebrafish were determined. Thus, thoracic kyphosis should be less than 30° in the sagittal plane and less than 10° in the coronal plane, in keeping with the definition of scoliosis in humans [19]. The high correlation coefficient between the values obtained by the two independent observers indicates good reproducibility. We believe that the parameters defined in this study hold promise for characterising spinal deformities in zebrafish according to the Lenke classification, which is the current reference standard for adolescent idiopathic scoliosis. That all six curve types defined by Lenke can be determined in the zebrafish should facilitate evaluations of phenotypic concordance with humans [20,21]. However, the absence of a pelvis in fish precludes the sagittal alignment assessment needed to determine the modifiers in the Lenke classification.

The limitations of this study include the number of animals, which was kept small to optimise animal welfare; the use of animals free of spontaneous deformities, requiring the induction of deformities for the study; and the unfeasibility of evaluating the inter-vertebral discs in addition to the vertebrae. Adding magnetic resonance imaging may help to overcome this last limitation in the future.

In conclusion, this work describes a new μCT method for evaluating the zebrafish spine based on recognised orthopaedic parameters. It should improve communication between clinicians and researchers during the design of future studies. The use of μCT seems indispensable for evaluating the zebrafish skeleton.

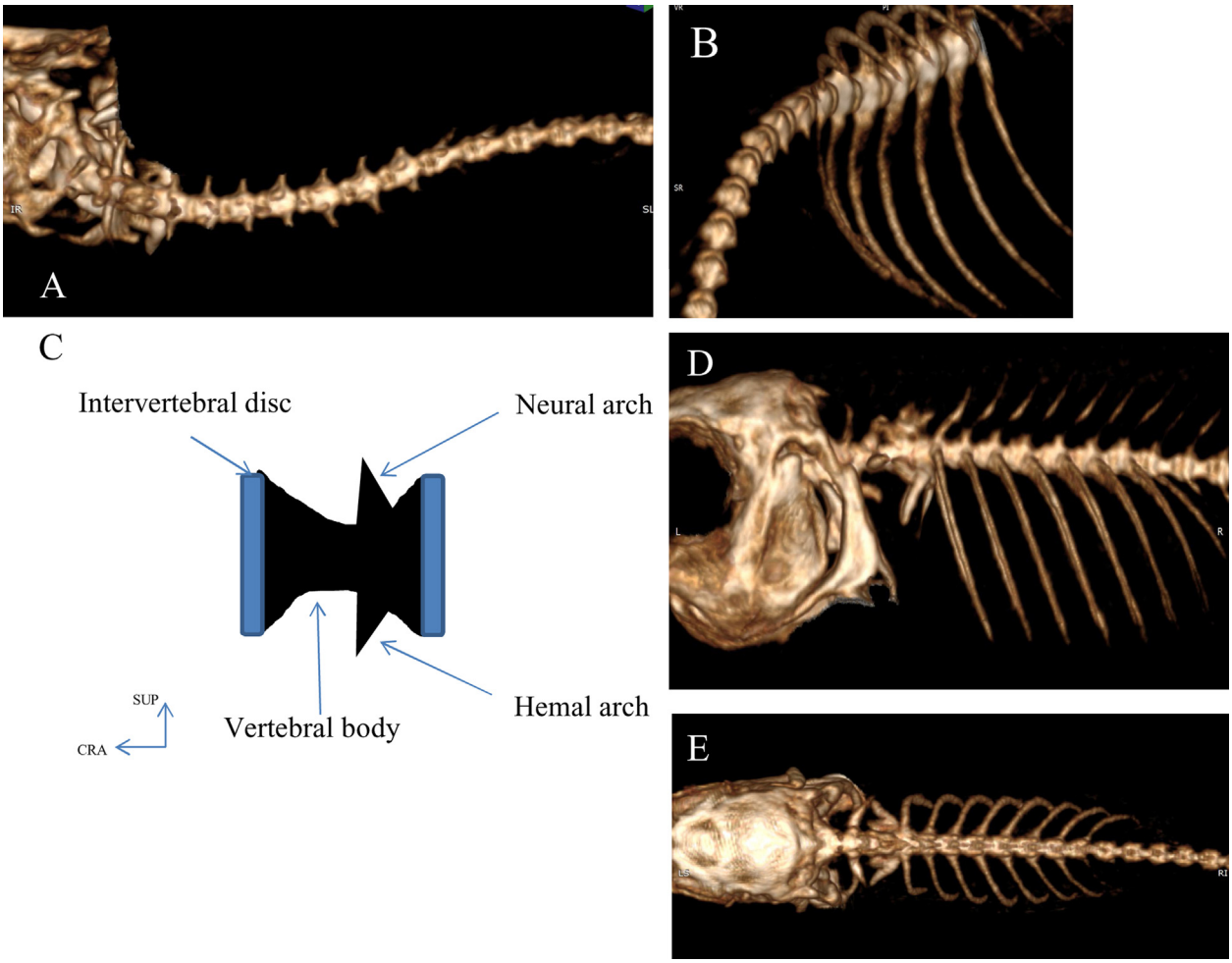

Fig. 7. Morphological evaluation of the spine. A and B. Evaluation of experimentally induced curves; absence of vertebral deformities. C. Diagram of the structure of a zebrafish vertebra. D and E. Sagittal and coronal views showing the cervical segment of the spine. SUP: superior; CRA: cranial.

Disclosure of interest

The authors declare that they have no competing interest.

Funding

This study was funded by a Master's II research grant from the SoFCOT (Société Française de Chirurgie Orthopédique et Traumatologie) awarded to Laura Marie-Hardy.

Contributions

LMH acquired and evaluated the images and wrote the manuscript.

MK independently recorded the μCT measurements for the reproducibility study.

LS acquired the images and helped to set up the study protocol.

HPM revised the manuscript.

Acknowledgement

We thanks the SOFCOT for her support.

References

[1] Howe K, Clark MD, Torroja CF, Torrance J, Berthelot C, Muffato M, Collins JE, et al. The zebrafish reference genome sequence and its relationship to the human genome. Nature 2013;496:498–503.
[2] Ministère de l»Enseignement supérieur de la Recherche et de l»Innovation. Enquête statistique sur l'utilisation des animaux à des fins scientifiques; 2014.
[3] Tavares B, Santos Lopes S. The importance of Zebrafish in biomedical research. Acta Med Port 2013;26:583–92.
[4] Jones RW, Stout MG, Reich H, Huffman MN. Cytotoxic activities of certain flavonoids against zebra-fish embryos. Cancer Chemother Rep 1964;34:19–20.
[5] Zheng X, Sun X, Qiu Y, Zhu ZZ, Bin W, Ding YT. Q, et al. A porcine early-onset scoliosis model created using a posterior mini-invasive method: a pilot study. J Spinal Disord Tech 2014;27:E294–300.
[6] Wu T, Sun X, Zhu Z, Yan H, Guo J, Cheng JC, et al. Role of enhanced central leptin activity in a scoliosis model created in bipedal amputated mice. Spine (Phila Pa 1976) 2015;40:E1041–5.
[7] Ouellet J, Odent T. Animal models for scoliosis research: state of the art, current concepts and future perspective applications. Eur Spine J 2013;22(Suppl 2):S81–95.
[8] Sternberg JR, Prendergast A, Brosse L, Cantaut-Belarif Y, Boccara C, Okamoto H, et al. Pkd2l1 is required for mechanoception in cerebrospinal fluid-contacting neurons and maintenance of spine curvature. Nat Commun 2018;9:3804.
[9] Ogura Y, Kou I, Miura S, Takahashi A, Shukunami C, Kamatani Y, et al. A Functional SNP in BNC2 is associated with adolescent idiopathic scoliosis. Am J Hum Genet 2015;97:337–42.
[10] Hayes M, Gao X, Yu LX, Paria N, Henkelman RM, Wise CA, et al. ptk7 mutant zebrafish models of congenital and idiopathic scoliosis implicate dysregulated Wnt signalling in disease. Nat Commun 2014;5:4777.

[11] Grimes DT, Boswell CW, Morante NF, Henkelman RM, Burdine RD, Ciruna B, et al. Zebrafish models of idiopathic scoliosis link cerebrospinal fluid flow defects to spine curvature. Science 2016;352:1341–4.
[12] Boswell CW, Ciruna B. Understanding idiopathic scoliosis: A new zebrafish school of thought. Trends Genet 2017;33:183–96.
[13] Gray RS, Wilm TP, Smith J, Bagnat M, Dale RM, Topczewski J, et al. Loss of col8a1a function during zebrafish embryogenesis results in congenital vertebral malformations. Dev Biol 2014;386:72–85.
[14] Gavaia PJ, Sarasquete C, Cancela ML. Detection of mineralized structures in early stages of development of marine Teleostei using a modified alcian blue-alizarin red double staining technique for bone and cartilage. Biotech Histochem 2000;75:79–84.
[15] Salgado D, Marcelle C, Currie PD, Bryson-Richardson RJ. The Zebrafish Anatomy Portal: a novel integrated resource to facilitate zebrafish research. Dev Biol 2012;372:1–4.
[16] Bird NC, Hernandez LP. Building an evolutionary innovation: differential growth in the modified vertebral elements of the zebrafish Weberian apparatus. Zoology 2009;112:97–112.
[17] Hur M, Gistelinck CA, Huber P, Lee J, Thompson MH, Monstad-Rios AT, et al. MicroCT-based phenomics in the zebrafish skeleton reveals virtues of deep phenotyping in a distributed organ system. Elife 2014;6:e26014.
[18] Charles JF, Sury M, Tsang K, Urso K, Henke K, Huang Y, et al. Utility of quantitative micro-computed tomographic analysis in zebrafish to define gene function during skeletogenesis. Bone 2017;101:162–71.
[19] Morin-KensickiE, Melancon M, Eisen J. Segmental relationship between somites and vertebral column in zebrafish. Development 2002;129:3851–60.
[20] Lenke LG, Betz RR, Clements D, Merola A, Haher T, Lowe T, et al. Curve prevalence of a new classification of operative adolescent idiopathic scoliosis: does classification correlate with treatment? Spine (Phila Pa 1976) 2002;27:604–11.
[21] Hoashi JS, Cahill PJ, Bennett JT, Samdani AF. Adolescent scoliosis classification and treatment. Neurosurg Clin N Am 2013;24:173–83.